Electronic Supplementary Material (ESI) for Journal of Materials Chemistry A.

Supporting information

Colossal permittivity with ultralow dielectric loss in In+Ta co-doped rutile TiO_2

Wen Dong[1], Wanbiao Hu[1], Terry Frankcombe[2], Dehong Chen[1], Chao Zhou[3], Zhenxiao Fu[3], Ladir Cândido[4], Guoqiang Hai[5], Hua Chen[6], Zhipu Liu[7], Yongxiang Li[7], Ray Withers[1] and Yun Liu[1,]*

[1]Research School of Chemistry, the Australian National University, ACT 2601, Australia

[2]School of Physical, Environmental and Mathematical Sciences, The University of New South Wales, Canberra, ACT 2601, Australia.

[3]Fenghua Advanced Technology Holding Co. Ltd., China

[4]Instituto de Física, Universidade Federal de Goiás, 74001-970, Goiânia, GO, Brazil

[5]Instituto de Física de São Carlos, Universidade de São Paulo, 13560-970, São Carlos, SP, Brazil

[6]Centre for Advanced Microscopy, The Australian National University, ACT 2601, Australia

[7]The Key Lab of Inorganic Functional Materials and Devices, Shanghai Institute of Ceramics, Chinese Academy of Sciences, Shanghai 200050, China

*To whom the correspondence should be addressed: yun.liu@anu.edu.au

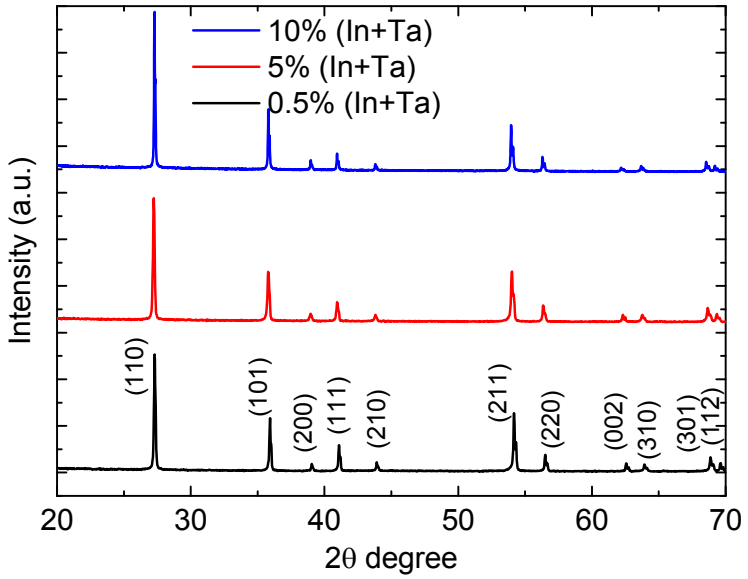

Fig. S1 XRD patterns of the synthesized In+Ta co-doped TiO_2 samples with different co-doping levels (0.5%, 5% and 10%). All the samples were of pure rutile TiO_2 phase.

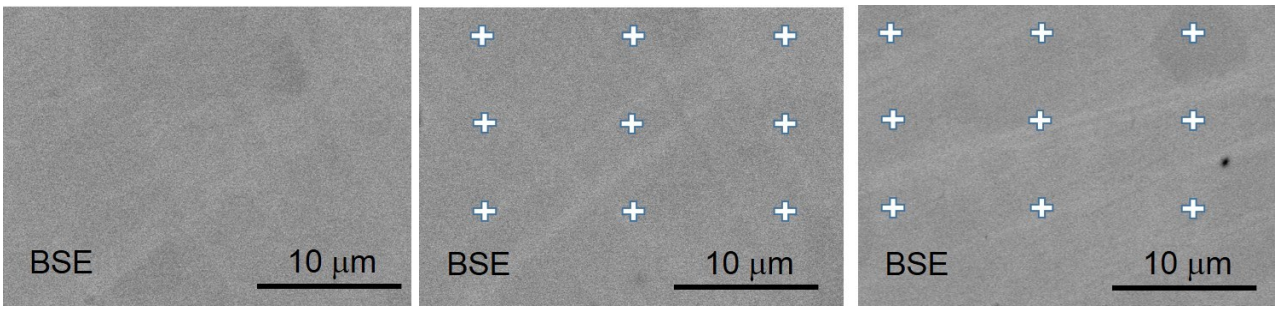

Fig. S2 The backscattering electron (BSE) images of (In, Ta) co-doped TiO_2 with nominal co-doping levels of 0.5%, 5%, and 10% from left to right, respectively. The white "+" symbols labeled in the image are the nine points that are used to collect EDS spectra to determine the average In:Ta:Ti ratio to the total cation, and the homogeneity of element distribution. The BSE images do not show any inhomogeneous element distribution for those samples in the measureable resolution. The EDS spectra were collected at nine points to indicate the differentiation of In, Ta and Ti distribution and experimentally determine the average In:Ta:Ti ratio to the total cation. Note that since the detected element distribution for the sample 0.5% co-doping level is within the error limit range of the EDS technique, the resultant In:Ta:Ti ratios for the samples with co-doping level of 5% and 10% are only presented, which are 0.025(±0.001):0.026(±0.001):0.949(±0.001) and 0.050(±0.002):0.051(±0.003):0.899(±0.001), respectively, clearly showing the average ratio is in a good consistent with the nominal ratio of 0.025:0.025:0.950 and 0.05:0.05:0.900. There is no inhomogeneous chemical distribution observed in all samples.

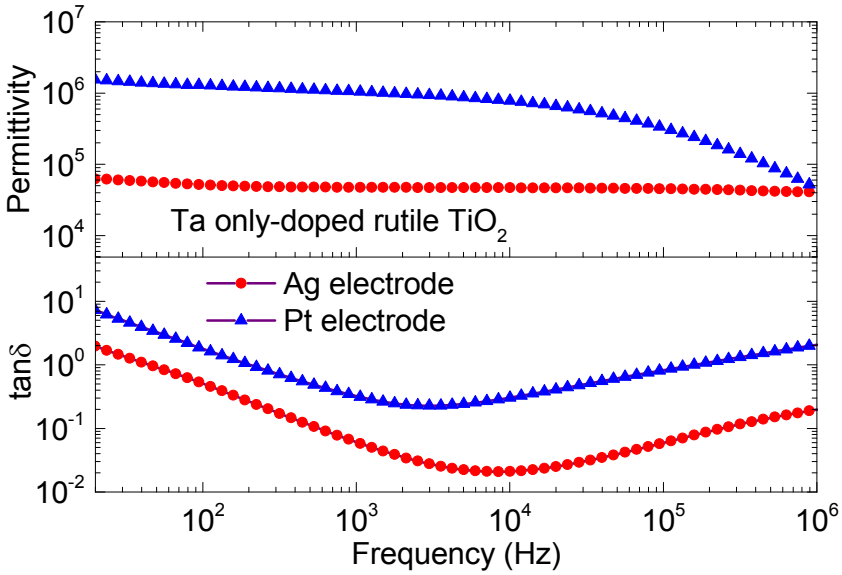

Fig. S3 Frequency-dependent dielectric permittivity and loss (tan δ) of the Ta-only doped rutile TiO_2 samples with Ag and Pt electrodes, where 0.25% Ti^{4+} were replaced by Ta^{5+}. The surface effect can be evidently observed in the Ta-only doped rutile TiO_2 , accompanying with a high dielectric loss.

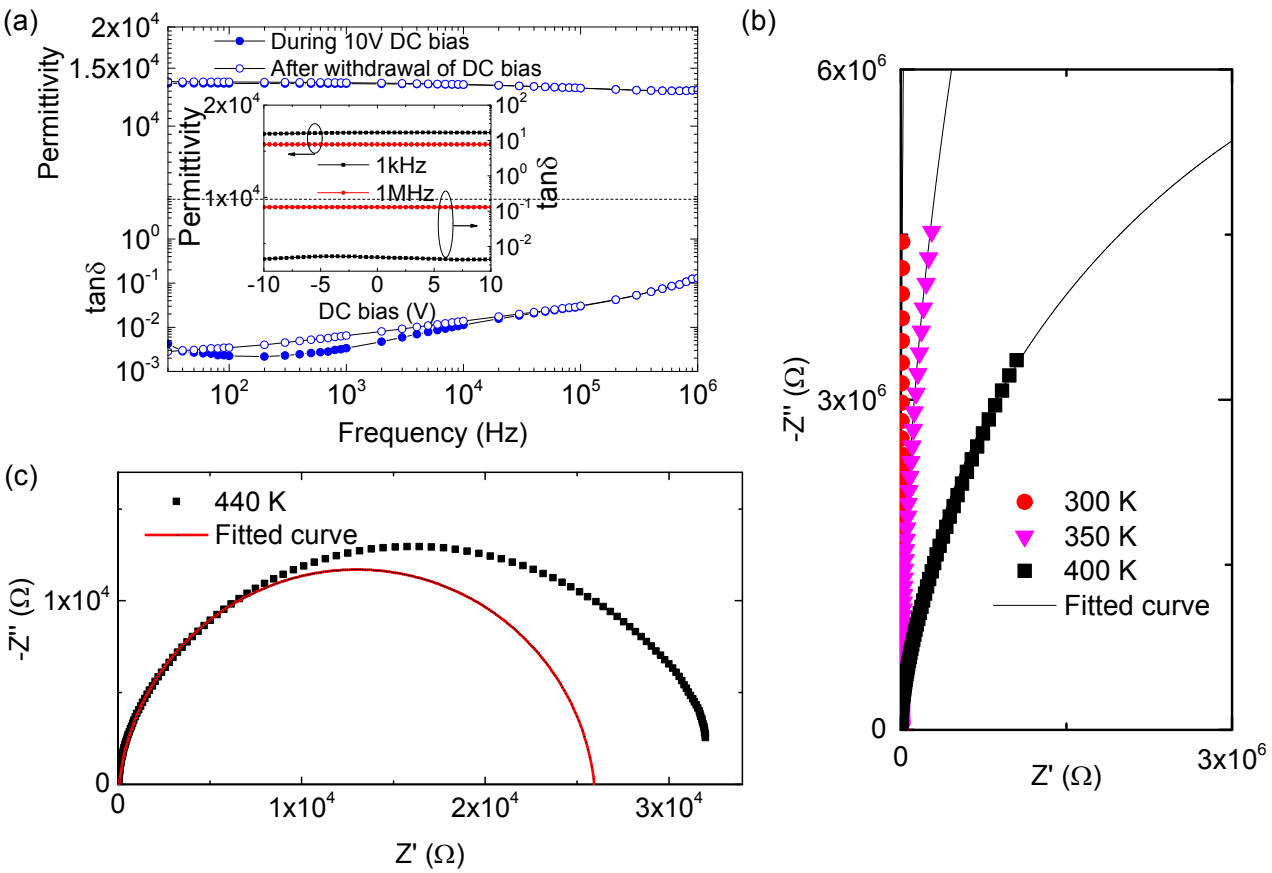

Fig. S4 (a) Frequency-dependent dielectric properties measured under 10V DC bias voltage and after withdrawal of the DC bias. Inset image is the relationship between the applied DC bias voltages and the dielectric properties measured at 1 kHz and 1 MHz, respectively. (b) and (c) complex impedance plots [Z'(ω)-Z"(ω)] (solid symbol) of 0.5% In+Ta co-doped rutile TiO_2 measured from 300 K to 450 K, and corresponding fitting results (solid lines) using Cole-Cole model. To explore the possibility of IBLC, we measured the dielectric properties under an applied direct current (DC) bias. The measurements were carried out on samples with Ag electrode after PA. Fig. S4a shows the measured room temperature, frequency-dependent permittivity and loss tangent curves under 10V DC bias. The permittivity remains nearly unchanged with and without the DC bias, respectively. Similarly, tan δ shows no obvious change in the higher frequency region (>10 kHz) but does not fully recover in the low frequency region (<10 kHz) after withdrawal of the DC bias. The difference of the tan δ in the low frequency range may due to limited space charge within the materials. There is no noticeable voltage dependency of the permittivity and loss tangent at both measured frequencies. In addition, the impact of DC voltages (from -10V to 10V) on the dielectric properties of the 0.5% In+Ta co-doped rutile TiO_2

is also investigated at 1 kHz and 1MHz frequencies, respectively. Again there is no noticeable voltage dependency of the permittivity and loss tangent at both measured frequencies. The tan δ measured at 1 kHz slightly change when the DC voltage is applied, but the relative amplitude of change is still less than 10%. This slightly change may also due to the limited space charge. These results differ from interfacial polarization dominated systems, in which numerous space charges were accumulated at interfacial region, resulting in significant increase of permittivity, dielectric loss or current when a small DC bias is applied.[1-3] The complex impedance spectra measured from 300 K and 400 K as shown in Fig. S4b can be well fitted using only one parallel RQ element since only an essentially linear arc with a high frequency near-zero intercept is observed from each complex impedance plot. The fitting results in the temperature range of 300~400 K suggest that the complex impedance contains only one component. Thus the intra-grain contribution can be considered to be the source of the colossal permittivity.[4] In contrast, the spectrum collected at 450 K cannot be fitted by using only one parallel RQ element, but requires two connected in series i.e. $(R_gQ_g)(R_{gb}Q_{gb})$. Here, R_g and R_{gb} represent the grain and grain boundary resistances, respectively. Q_i (i=g, gb) is the corresponding constant phase element.[5] These results indicate that the interfacial effect isn't observed at temperatures below 400 K but appears only above 450 K. This is in good agreement with the (only high-temperature) Maxwell-Wagner type and also consistent with the result in Fig. 3a. Therefore, the CP behavior in the 0.5% In+Ta co-doped rutile TiO_2 samples should be attributed to the quasi-intrinsic EPDD in grain interior.

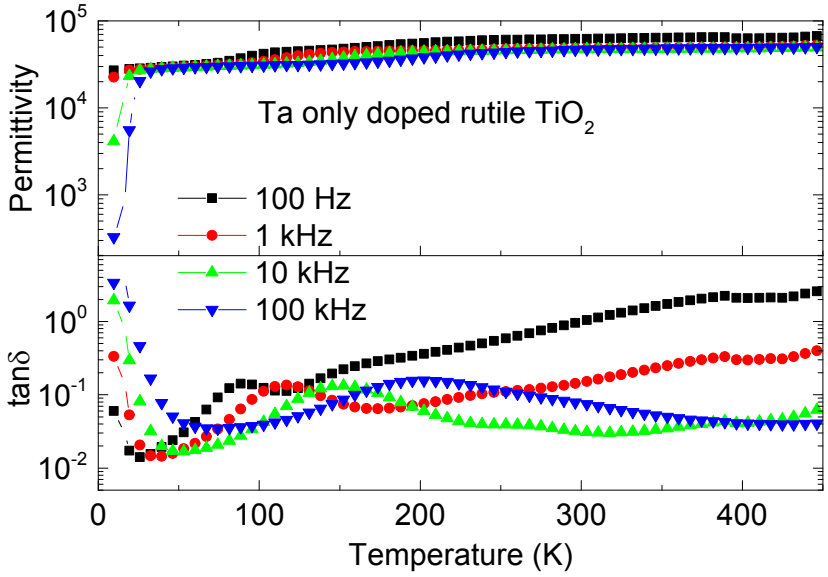

Fig. S5 Temperature dependences of dielectric property of Ta-only doped rutile TiO_2 (where 0.25% Ti^{4+} were replaced by Ta^{5+}) with Ag electrode. Both the dielectric permittivity and loss show the distinct temperature-dependence behaviors.

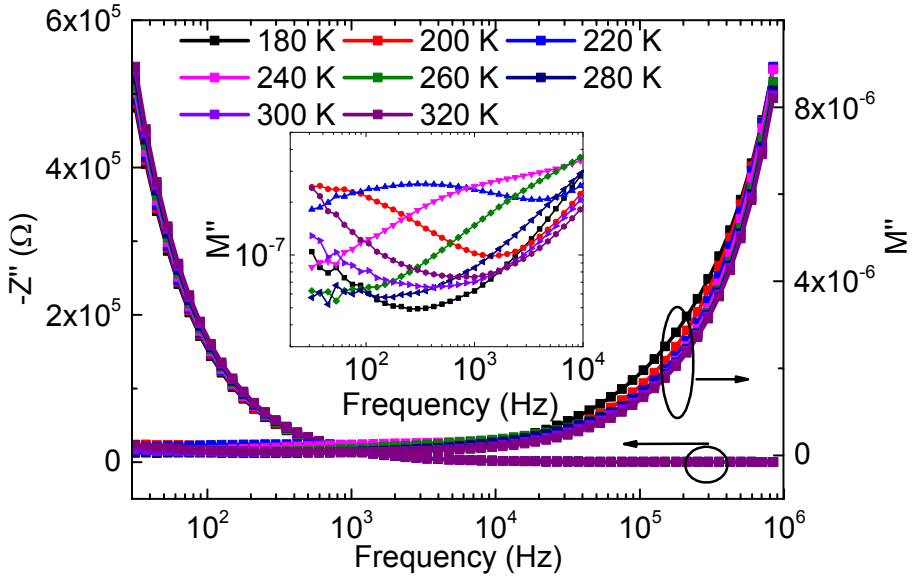

Fig. S6 Impedance and modulus plots for 0.5% In+Ta co-doped rutile TiO_2 samples measured at selected temperature points in the temperature range 180~320 K. Inset shows a magnified region in frequency range 20~10 kHz for modulus. For the relaxation region in 200~300 K, SBLC and IBLC can be excluded since the dielectric relaxation is almost independent of electrode and voltage, respectively. Therefore, this relaxation should be originated from the bulk of the sample. In addition to the temperature spectrum, impedance and modulus measurements were carried out to further investigate the polarization mechanism responsible for the dielectric relaxation region in 200~300 K. Electric modulus is an effective way to investigate defect relaxation in polycrystalline ceramics since the transport of mobile charge carriers is related to the relaxation behavior in both impedance and modulus. The peak height of the impedance Z'' is proportional to "R" for the element, while M" is inversely proportional to "C" for the element. The modulus plots can pick out the grain response while the impedance plot can pick out the surface and grain effect induced resistance. Thus, the difference of the M" and Z" curves will dependent on the electrical homogeneousness of the ceramic materials, which is related to the long-range or short range transport behavior of carriers.[6-8] Fig. S6 indicates a sharp increase in the imaginary part of the modulus at high frequency region, whereas no response is found in impedance at high frequency region. Meanwhile, in low frequency region, a slight response in modulus (inset image) and a sharp increase of impedance can be visible as the frequency decreases, in which both curves are not overlapped. These results indicate that both bulk responses of the 0.5% In+Ta co-doped rutile TiO_2 is due to localized relaxation rather than long range transport of carriers.

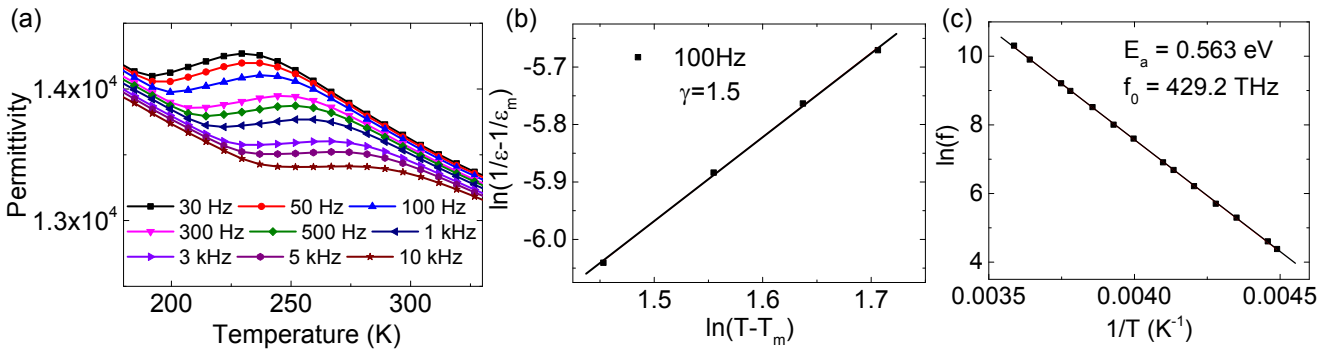

Fig. S7 (a) Dielectric permittivity for 0.5% In+Ta co-doped rutile TiO_2 over temperature range 180~325 K. (b) Plotting of $\ln(1/\varepsilon-1/\varepsilon_m)$ vs $\ln(T-T_m)$ measured at 100 Hz. (c) Plot of ln f versus 1/T for 0.5% In+Ta co-doped rutile TiO_2.

Fig. S7a shows the relaxor-type relaxation observed within the temperature range 200~300 K for 0.5% In+Ta co-doped rutile TiO_2. It can be seen that at higher frequencies the peaks are broader (diffuse). A decrease in the maximum dielectric permittivity value ε_m is observed with increasing frequency in addition to an increase in the temperature position T_m.

A modified empirical quadratic Curie-Weiss law was used to describe the diffuseness of the relaxor-type state, given by

$$1/\varepsilon=1/\varepsilon_m+(T-T_m)^{\gamma}/C, \quad (1)$$

where ε_m is the maximum permittivity value at T_m, C is Curie constant and the degree of diffuseness of the permittivity peak. The exponent γ was obtained by fitting $\varepsilon(T)$ data on the high temperature side of T_m in the range of T_m+25 K~ T_m+50 K. $\ln(1/\varepsilon-1/\varepsilon_m)$ was plotted against $\ln(T-T_m)$ measured at 100 Hz (Fig. S7b). A diffuseness γ of ~1.5 was obtained, indicating a relaxor relaxation behavior.[9,10] This result support the relaxor-type behavior for the dielectric relaxation corresponds to 200~300 K region. Fig. S7c presents the linear fitting of the ln(f) vs 1/T for the relaxation peaks from dielectric loss curves, an activation energy of 0.562 eV activation energy followed by an engine frequency value of 429 THz were obtained using Arrhenius equation. The high activation energy combined with the THz level Eigen-frequency value also support the relaxor type relaxation from cation move of center.

References

1 G. Z. Liu, C. Wang, C. C. Wang, J. Qiu, M. He, J. Xing, K. J. Jin, H. B. Lu, G. Z. Yang, *Appl. Phys. Lett.* 2008, **92**, 122903.

2 P. Lunkenheimer, R. Fichtl, S. G. Ebbinghaus, A. Loidl, *Phys. Rev. B* 2004, **70**, 172102.

3 J. Li, F. Li, C. Li, G. Yang, Z. Xu, S. Zhang, *Sci. Rep.* 2015, **5***,* 8295.

4 J. Yang, J. He, J. Y. Zhu, W. Bai, L. Sun, X. J. Meng, X. D. Tang, C. G. Duan, D. Rémiens, J. H. Qiu, J. H. Chu, *Appl. Phys. Lett.* 2012, **101**, 222904.

5 S. M. Haile, D. L. West, J. Campbell, *J. Mater. Res.* 1998, **13**, 1576-1595.

6 W. Cao, R. Gerhardt, *Solid State Ionics* 1990, **42**, 213-221.

7 R. Gerhardt, *J. Phys. Chem. Solids* 1994, **55**, 1491-1506.

8 W. Hu, L. Li, G. Li, Y. Liu, R. L. Withers, *Sci. Rep.* 2014, **4**, 6582.

9 A. K. Axelsson, Y. Pan, M. Valant, P. M. Vilarinho, N. M. Alford, *J. Appl. Phys.* 2010, **108**, 064109.

10 V. J. Minkiewicz, Y. Fujii, Y. Yamada, *J. Phys. Soc. Jpn.* 1970, **28**, 443-450.